Proceedings of the International Workshop "Oxide Materials for Electronic Engineering" (OMEE-2009), Lviv 2009

The Passively *Q*-switched Microchip Nd:YAG Laser Optimization for Rangefinder Applications

O. Buryy[a,*], A. Iznin[b], I.I. Syvorotka[b], D. Sugak[b], S. Ubizskii[a] and M. Vakiv[b]

[a]Institute of Telecommunications, Radioelectronics and Electronic Engineering

Lviv Polytechnic National University, Bandery 12, 79046 Lviv, Ukraine

[b]Scientific Research Company "Carat", Stryjska 202, 79031 Lviv, Ukraine

The problem of Q-switched microchip Nd^{3+}:YAG/Cr^{4+}:YAG laser optimization is considered. In accordance with requirements of laser location, the optimization consists in determination of such values of the saturable absorber (Cr^{4+}:YAG) thickness, the output laser mirror reflectivity and the pumping power, that ensure the generation of the sufficiently short (≈ 0.5 ns) laser pulses at the repetition rate of about 10 kHz and the peak power of about 1 kW or higher. Firstly, the dependences of the laser radiation parameters on the constructive ones are analyzed in the frames of Xiao-Bass model of Q-switched microchip laser. The obtained dependences are used for laser optimization. As it is shown, the parameters of laser radiation close to predominating ones are achieved at the absorber thickness of 140 μm, the output mirror reflectivity of 0.97 and the pumping power of 2.5 W.

PACS numbers: 42.60.Gd

1. Introduction

Recently, the Q-switched microchip lasers are widely investigated and used as compact, relatively high-power coherent radiation sources for the needs of ranging, sensing, material treatment. Such a laser consists of the generating (usually Nd^{3+}:YAG) crystal with the Cr^{4+}:YAG saturable absorber layer and the input and output mirrors formed on the cavity faces. The ability to the saturable absorption near 1 μm is provided by the ${}^3A_2 \rightarrow {}^3T_2$ and ${}^3T_2 \rightarrow {}^3T_1$ transitions of the tetrahedrally coordinated Cr^{4+} ions, referred hereafter also as phototropic centers.

Here we consider the problem of the Q-switched microchip laser optimization for rangefinder applications. Usually, they require the pulse laser radiation with sufficiently low duration of the laser pulse (≈ 0.5 ns or lower) at the repetition rate about 10 kHz, and the peak power about 1 kW or higher (i.e., the energy in the laser pulse about 0.5 μJ or higher). The desirable characteristics of laser radiation can be achieved by variation of the laser design parameters: the thickness of the generating medium and the absorber, the concentration of phototropic centers, the output mirror reflectivity, as well as the pumping power and the radius of the pumping beam. The determination of the optimal laser parameters in our work is based on solutions of the rate equations system describing the process of laser generation. Then, dependences of the laser radiation parameters on the design ones, obtained from the solutions of this system, are used for optimization of the Q-switched microchip Nd^{3+}:YAG/Cr^{4+}:YAG (Nd:YAG/Cr:YAG) laser.

* corresponding author; e-mail: crystal@polynet.lviv.ua

2. Modeling of the Q-switched microchip Nd:YAG/Cr:YAG laser

2.1. Main expressions

Modeling of passively Q-switched microchip Nd:YAG/Cr:YAG laser is based on the Xiao–Bass model [1–3] represented by a system of differential equations describing the dynamics of the inversion in the generating medium, the absorption in Cr:YAG and the photons generation

$$\begin{cases} \dfrac{\mathrm{d}n_\mathrm{g}}{\mathrm{d}t} = R - \dfrac{\sigma_\mathrm{g} c_0}{V'} n_\mathrm{g} q - \dfrac{n_\mathrm{g}}{\tau_\mathrm{g}}, \\ \dfrac{\mathrm{d}n_\mathrm{a}}{\mathrm{d}t} = -\dfrac{\sigma_\mathrm{a1} c_0}{V'} n_\mathrm{a} q + \dfrac{n_\mathrm{a0} - n_\mathrm{a}}{\tau_\mathrm{a}}, \\ \dfrac{\mathrm{d}q}{\mathrm{d}t} = \Big(2 n_\mathrm{g} \sigma_\mathrm{g} l_\mathrm{g} - 2 n_\mathrm{a} \sigma_\mathrm{a1} l_\mathrm{a} \\ \quad -2\left(n_\mathrm{a0} - n_\mathrm{a}\right) \sigma_\mathrm{a2} l_\mathrm{a} - 2\gamma\Big) \dfrac{q}{t_\mathrm{r}} \\ \quad +\varepsilon\left(n_\mathrm{g} + n_\mathrm{g0}\right) c_0 \sigma_\mathrm{g} l_\mathrm{g} / l'. \end{cases} \tag{1}$$

Here $c_0 = 3\times10^8$ m/s, n_{g0} is the activator (Nd^{3+}) concentration (usually n_{g0} is about 1 at.%), n_{a0} is the concentration of the tetrahedrally coordinated Cr^{4+} ($n_{a0} \approx 10^{17}$–10^{19} cm^{-3}), n_g is the inversion in the generating medium, n_a is the concentration of the Cr^{4+} (tetra) ions on the ground level, σ_g is the laser transition cross-section ($\sigma_g = 3.5 \times 10^{-19}$ cm^2 for Nd:YAG [4]), σ_{a1}, σ_{a2} are the cross-sections of the ground state (GSA) and excited absorption state (ESA) of Cr^{4+} (tetra), τ_g is the upper laser level lifetime ($\tau_g = 0.23$ ms), τ_a is the lifetime of the Cr^{4+}(tetra) excited ${}^3T_2$ level ($\tau_a = 3.5$ μs), l_g is the generating medium length ($l_g \approx 1$ mm), l_a is the absorber thickness ($l_a \approx 10$–250 μm), $l' = nl$ is the optical length of the resonator (n is the refractive index, $n = 1.816$ for YAG; $l = l_g + l_a$ is the resonator length), $t_r = 2l'/c_0$ is the time of double passing of the resonator, $R = \frac{\eta P_p}{V h \nu_p}$ (P_p is the pumping power, η is the pumping efficiency, $V = \pi r_p^2 l_g$, r_p is the pumping beam radius, ν_p is the frequency of the pumping radiation), ε is the dimensionless coefficient characterising the relative power of the spontaneous radiation ($\varepsilon = 10^{-13}$ [5]), V' is the effective mode volume ($V' = (l'/l_a)V_g$, V_g is the mode volume, $V_g = Al_g$, where $A = 0.5\pi r_l^2$, r_l is the laser beam radius (by intensity), the multiplier 0.5 appears because the laser mode has got the standing wave character [4]), γ is the losses during one passing of the resonator ($\gamma = \gamma_i - 0.5 \ln R_1 R_2$, γ_i is the summarized diffraction and non-active absorption losses are the generating medium and the absorber; it must be mentioned that the Fresnel number for microchip lasers is high (≈ 400), so the diffraction losses is low and we may put $\gamma_i = \alpha l$, α is the absorption coefficient for non-active losses, $\alpha \approx 0.005$ cm^{-1} for YAG [5], R_1, R_2 are the reflectivities of input ($R_1 \approx 1$) and output mirrors at the laser wavelength (1.064 μm)), q is the quantity of photons in the resonator concerned with laser output power by the expression $P(t) = \frac{h\nu}{t_r} \ln(\frac{1}{R_2}) q(t)$, ($\nu$ is the laser radiation frequency). The energy in the laser pulse can be calculated as $E = \int P(t)\, dt$, where the integral limits are determined by the pulse duration.

Here we consider both the numerical solutions obtained by the fourth order Runge–Kutta technique, as well as the rough analytical solutions of Eqs. (1). The last ones may be obtained if the terms describing the pumping and the spontaneous transitions will be neglected [3]. Particularly, for the peak power and the energy one can obtain

$$P_{max} = \frac{h\nu A l}{t_r} \ln \frac{1}{R_1 R_2} \times \left\{ n_{gi} - n_{gt} - \frac{n_{a0} l_a}{l_g} \left(1 - \frac{\sigma_{a2}}{\sigma_{a1}}\right) \left[1 - \left(\frac{n_{gt}}{n_{gi}}\right)^{\sigma_{a1}/\sigma_g}\right] - \frac{\alpha l - \ln(R_1 R_2) + \sigma_{a2} l_a n_{a0}}{\sigma_g l_g} \ln\left(\frac{n_{gi}}{n_{gt}}\right) \right\}, \quad (2)$$

$$E = \frac{h\nu A}{2\sigma_g} \ln\left(\frac{1}{R_1 R_2}\right) \ln\left(\frac{n_{gf}}{n_{gi}}\right), \quad (3)$$

where n_{gi} is the inversion in the generating medium before laser pulse irradiation, i.e., at the moment when the amplification in the active medium is equal to the losses

$$\sigma_g l_g n_{gi} = \sigma_{a1} l_a n_{a0} + \alpha l - 0.5 \ln(R_1 R_2), \quad (4)$$

n_{gt} is the inversion in the generating medium at the moment when the power of the laser radiation has got a maximum; this inversion can be determined from the equation

$$\sigma_g l_g n_{gt} - \alpha l + 0.5 \ln(R_1 R_2) - \sigma_{a2} l_a n_{a0} - (\sigma_{a1} - \sigma_{a2}) l_a n_{a0} \left(\frac{n_{gt}}{n_{gi}}\right)^{\sigma_{a1}/\sigma_g} = 0, \quad (5)$$

n_{gf} is the residual inversion in the generating medium that can be calculated from [3]:

$$n_{gi} - n_{gf} - n_{a0} \frac{l_a}{l_g} \left(1 - \frac{\sigma_{a2}}{\sigma_{a1}}\right) \left[1 - \left(\frac{n_{gf}}{n_{gi}}\right)^{\sigma_1/\sigma_a}\right] - \frac{\alpha l - 0.5 \ln(R_1 R_2) + \sigma_{a2} l_a n_{a0}}{\sigma_g l_g} \ln\left(\frac{n_{gi}}{n_{gf}}\right) = 0. \quad (6)$$

The duration of the laser pulse t_i is assumed to be estimated as:

$$t_i = \frac{E}{P_{max}}. \quad (7)$$

The repetition rate F is the inverse to time interval of inversion increasing from n_{gf} to n_{gi} [6]:

$$F = \frac{1}{\tau_g} \left[\ln\left(\frac{n_{gf} - R\tau_g}{n_{gi} - R\tau_g}\right)\right]^{-1}. \quad (8)$$

2.2. The parameters of the laser crystal

For optimization we used the starting parameters corresponding to ones of the experimental Nd:YAG/Cr:YAG microchip laser elaborated at SRC "Carat", see Table I.

The problem of the Nd:YAG/Cr:YAG microchip laser optimization becomes rather complicated by the uncertainty in the values of the GSA and ESA cross-sections of Cr^{4+} (tetra) ions σ_{a1}, σ_{a2}. The values of these parameters obtained in different works are shown in Table II. The values of the cross-sections σ_{a1}, σ_{a2} calculated from the results of [11] are significantly higher than the ones obtained in other works and, obviously, have got the artifact character. Also, the values obtained in [10] look as overestimated. Because of the uncertainty of the σ_{a1}, σ_{a2}, all calculations in the present work were carried out for three different sets of values. Each set was determined by the value of σ_{a1} obtained in [2–3, 8] and the cross-section σ_{a2} was determined by fitting of the experimental data for Nd:YAG/Cr:YAG laser (Table I). Such an approach bases on the fact that the precision of the experimental determination of the GSA cross-section σ_{a1} is higher than the one of ESA cross-section σ_{a2}. Indeed, as it follows from the data shown in Table II, the relative difference between the values of σ_{a1} obtained in [2, 8] is equal to 1.7, whereas the corresponding difference for σ_{a2} is two times higher. It must be mentioned that the values of σ_{a2} obtained by us are essentially higher than the ones indicated in [2, 3, 8]. Probably it is caused by peculiarities of the absorption medium used in this realization of the Nd:YAG/Cr:YAG laser, particularly, by using of epitaxial Cr:YAG film, not a bulk crystal. Besides σ_{a2}, other fitting parameters are the radii of the pumping r_p and the laser r_l beams. The obtained values of the fitting parameters are shown in Table III. The corresponding values of the laser radiation parameters, as well as the concentrations of the phototropic centers Cr^{4+}(tetra) determined as $n_{a0} = \alpha_0/\sigma_{a1}$, where α_0 is the initial absorption coefficient of the absorber at 1.064 μm, are also indicated in Table III. The value of the pumping beam radius obtained from the fitting is equal to 167–179 μm for different data sets and is higher than its experimental estimation, 75–100 μm. On the other hand, the obtained values of the laser radiation beam r_l (75–92 μm) are lower than the experimental value ($\approx$ 200 μm). This uncertainty is probably caused by the inaccuracy of the experimental estimations and, probably, by some limitations of the model (1).

TABLE I

Characteristics of the Nd:YAG/Cr:YAG microchip laser elaborated at SRC "Carat".

Parameter	Value
generating medium length l_g [mm]	1
absorber thickness l_a [mm]	0.065
transversal dimensions (square cross-section) [mm]	1.36
activator Nd^{3+} concentration, n_{g0} [at.%]	0.8–0.9
pumping wavelength λ_p [μm]	0.808
absorption coefficient of the generating medium at the pumping wavelength [cm^{-1}]	7
absorption coefficient of the absorber at the pumping wavelength [cm^{-1}]	8
incident pumping power P_p [W]	1.2
laser wavelength λ [μm]	1.064
initial absorption coefficient of the absorber at the laser wavelength α_0 [cm^{-1}]	20
reflectivity of the output mirror at the laser wavelength R_2	0.94
energy of the laser pulse E [μJ]	1.2
peak power of the laser pulse P_{max} [kW]	0.9
laser pulse duration t_i [ns]	1.36
repetition rate F [kHz]	9.8

TABLE II

The absorption cross-sections of Cr^{4+} (tetra) ions in YAG.

Value	Reference	Comments
$\sigma_{a1} = (0.7–1.0) \times 10^{-18}$ cm^2 $\sigma_{a2} = (0.85–2.95) \times 10^{-19}$ cm^2	[7]	Cr,Ca:YAG crystals
$\sigma_{a1} = 1.5 \times 10^{-18}$ cm^2 $\sigma_{a2} = 1.0 \times 10^{-19}$ cm^2	[2]	
$\sigma_{a1} = 2.5 \times 10^{-18}$ cm^2 $\sigma_{a2} = 3.0 \times 10^{-19}$ cm^2	[3]	Cr,Mg:YAG crystal
$\sigma_{a1} = 3.2 \times 10^{-18}$ cm^2, $\sigma_{a2} = 4.5 \times 10^{-19}$ cm^2	[8]	Cr,Ca:YAG crystal
$\sigma_{a1} = (3.93; 4.44; 4.52) \times 10^{-18}$ cm^2 $\sigma_{a2} = (1.5;\ 1.6) \times 10^{-19}$ cm^2	[9]	Cr,Mg:YAG crystals
$\sigma_{a1} = 7 \times 10^{-18}$ cm^2, $\sigma_{a2} = 2 \times 10^{-18}$ cm^2	[10]	
$\sigma_{a1} = 3.1 \times 10^{-17}$ cm^2 $\sigma_{a2} = 8.0 \times 10^{-18}$ cm^2	calculated from results of [11]	Cr,Mg:YAG epitaxial film

2.3. Dependences of the lasing characteristics upon laser construction parameters

In principle, the problem of microchip laser optimization can be solved by analytical or numerical calculations of the laser radiation parameters for the wide set of the constructive parameters, i.e., the output mirror reflectivity R_2, the generating medium and absorber thicknesses l_g and l_a, the phototropic centers concentration n_{a0}, and the pumping power P_p. However, this problem can be essentially simplified if the typical dependences of the laser radiation parameters on the constructive ones will be determined. For higher reliability all these dependences were obtained by numerical solving of the system (1) for data sets A–C from Table III.

The typical dependences of the laser radiation parameters on the phototropic centers concentration n_{a0} are shown in Fig. 1. The general trends of these dependences are the same for all data sets: the peak power and the energy of the laser pulse increase and the pulse duration and repetition rate decrease with increase of n_{a0}. At that, decrease of the pulse duration t_i is inessential at high enough values of n_{a0} (Fig. 1c), so the required duration (≈ 0.5 ns) cannot be achieved only by increase of the phototropic centers concentration. Besides, increase of n_{a0} may lead to repetition rate decreasing (Fig. 1d) out of the required values (about 10 kHz).

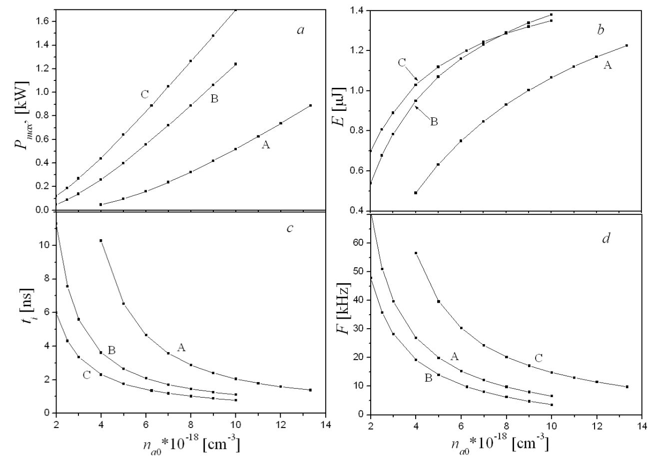

Fig. 1. Dependences of the peak power $P_{\max}$ (a), the energy E (b), the pulse duration t_i (c) and the repetition rate F (d) on the phototropic Cr^{4+} (tetra) centers concentration n_{a0}.

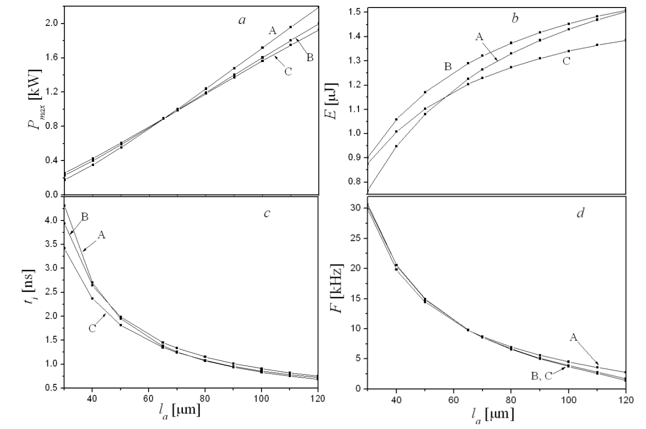

Fig. 2. Dependences of the peak power $P_{\max}$ (a), the energy E (b), the pulse duration t_i (c) and the repetition rate F (d) on the absorber thickness l_a.

The typical dependences of the laser radiation parameters on the absorber thickness l_a are shown in Fig. 2. As it is seen from Fig. 2, increasing of the absorber thickness leads to the changes analogously to the ones caused by increase of the phototropic centers concentration. It is directly seen from the expressions (2), (4)–(6), which contain the n_{a0} and l_a values only as the product. Though the absorber thickness l_a determines the resonator length $l = l_g + l_a$, under the condition $l_g \gg l_a$ (valid for microchip laser), the laser radiation parameters insignificantly depend on l_a via their contribution to l. Particularly, in [12] it is shown that the relative differences in the values of the pulse energies for microchip lasers with the same absorber initial transmission $T_0 = \exp(-\sigma_{a1} n_{a0} l_a)$ but with the different values of n_{a0} and l_a are in the limits of $\approx 10\%$.

Thus, the laser radiation parameters may be considered as dependent on the initial transmission of the absorber T_0 only, not on its thickness and Cr^{4+} (tetra) ions concentration separately. Further we will connect the changes of the initial transmission with the absorber thickness, because this parameter is better controlled than the phototropic centers concentration.

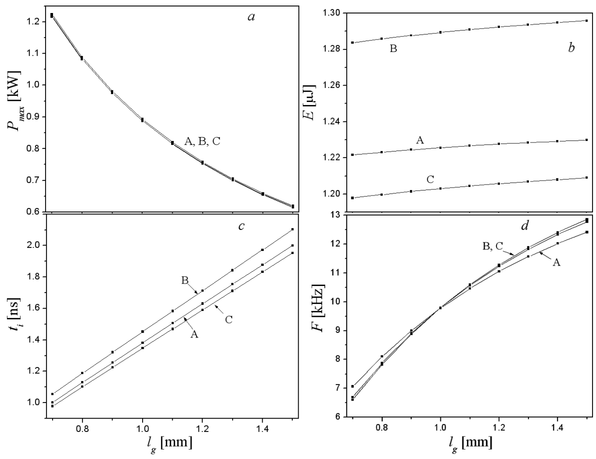

Fig. 3. Dependences of the peak power $P_{\max}$ (a), the energy E (b), the pulse duration t_i (c) and the repetition rate F (d) on the thickness of the generating medium l_g.

The typical dependences of the laser radiation parameters on the generating medium thickness l_g are shown in Fig. 3. As it is seen from Fig. 3, the changes of the laser radiation parameters caused by changing of the generating medium thickness are generally opposite to the ones caused by changing of the absorber thickness. Only the dependences of the energy of the laser pulse E on l_a and l_g have got the same character, however, the $E(l_g)$ dependence is essentially weaker than $E(l_a)$ one (Fig. 2b and Fig. 3b). Thus, because the analogous effect can be obtained due to the opposite variations of l_g and l_a, we do not consider the generating medium thickness as the optimization parameter. In all further calculations it will be fixed on the value $l_g = 1$ mm corresponding to the thickness of Nd:YAG substrate used in our experiments.

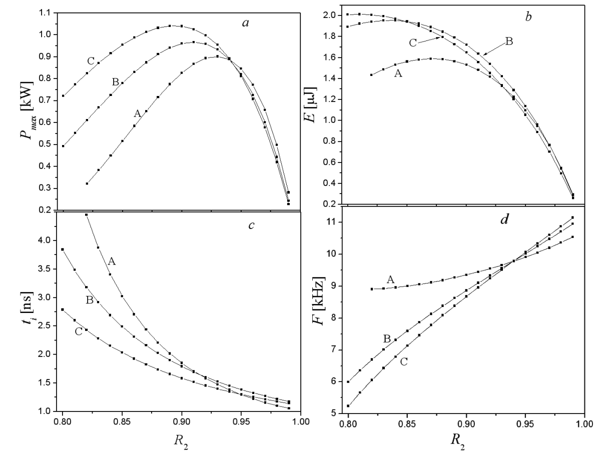

Fig. 4. Dependences of the peak power $P_{\max}$ (a), the energy E (b), the pulse duration t_i (c) and the repetition rate F (d) on the output mirror reflectivity R_2.

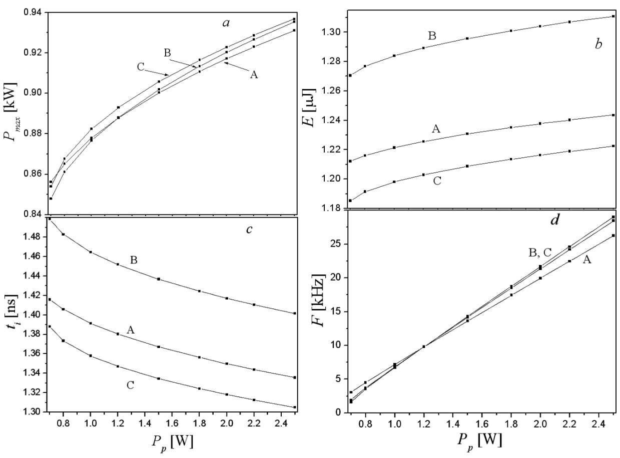

Fig. 5. Dependences of the peak power $P_{\max}$ (a), the energy E (b), the pulse duration t_i (c) and the repetition rate F (d) on the pumping power $P_{\rm p}$.

The typical dependences of the laser radiation parameters on the output mirror reflectivity R_2 are shown in Fig. 4. The maxima on the dependences of the peak power and the energy are typical for such dependences and correspond to the optimal values of the reflectivity. The duration of the laser pulse t_i decreases with increase of the reflectivity R_2 (Fig. 4c) that enables controlling the pulse duration by changing of R_2. The repetition rate increases with increase of the reflectivity (Fig. 4d). It must be mentioned that, in general, the $F(R_2)$ dependence has got more complicate character. As it was shown in [12], this dependence may have got a minimum caused by two opposite trends: decrease of the repetition rate due to increase of the inversion utilization factor and increase of the repetition rate due to the inversion accumulation rate $dn_{\rm g}/dt$ increasing with the increase of reflectivity R_2. So, at the values of the reflectivity accepted in this work we observe only the right part of $F(R_2)$ dependence.

The typical dependences of the laser radiation parameters on the pumping power $P_{\rm p}$ are shown in Fig. 5. As it is seen from Fig. 5a–c, the changes of the peak power, the energy and the duration of the laser pulse are insignificant if the pumping power changes are in the limit of 0.7–2.5 W. It also followed from the approximate expressions (2)–(7), which do not contain the dependences on the pumping power. The repetition rate depends on the pumping power practically linearly (Fig. 5d). Thus, the pumping power changing allows to obtain the required value of the repetition rate without considerable changes of the other parameters of the laser radiation.

3. The optimization of the microchip Nd:YAG/Cr:YAG laser

As it is mentioned above, the optimization of the microchip Nd:YAG/Cr:YAG laser for rangefinder applications consists in the determination of the construction (optimization) parameters that allows to ensure the laser pulse duration about 0.5 ns or lower, the repetition rate about 10 kHz and the peak power about 1 kW or higher, i.e., the energy in laser pulse about 0.5 μJ or higher. In accordance with the conclusions of the previous chapter, we use three optimization parameters: the absorber thickness $l_{\rm a}$, the output mirror reflectivity R_2 and the pumping power $P_{\rm p}$. At that, the essential methodological aspect of the optimization was minimizing of the influence of the uncertainty of absorption cross-sections $\sigma_{\rm a1}$, $\sigma_{\rm a2}$ values on the results of the optimization procedure. On the other words, the obtained optimal values of the $l_{\rm a}$, R_2 and $P_{\rm p}$ should not essentially differ for different data sets indicated in Table III.

The optimization was realized in the following sequence. Firstly, the pulse duration close to the required one ($\approx$ 0.5 ns) was ensured by fitting of the absorber thickness and the output mirror reflectivity. Then, the required value of the repetition rate ($\approx$ 10 kHz) was reached by fitting of the pumping power. The optimization of the peak power or energy was not carried out, because both these parameters remained in acceptable limits during the optimization of pulse duration and repetition rate. The obtained values of the optimization parameters and the corresponding parameters of the laser radiation are indicated in Table IV. As it is seen from Table IV, the obtained values of the optimization parameters are the same for all data sets and the parameters of radiation are close. Thus, the required parameters of the laser radiation can be achieved at the absorber thickness about 140 μm, the output mirror reflectivity about 0.97 and the pumping power about 2.5 W.

TABLE III

The parameters of the microchip Nd:YAG/Cr:YAG laser for different data sets.

Data set	$\sigma_{a1} \times 10^{18}$ [cm^2]	$\sigma_{a2} \times 10^{19}$ [cm^2]	r_p [μm]	r_l [μm]	$n_{a0} \times 10^{-18}$ [cm^{-3}]	P_{max} [kW]	E [μJ]	t_i [ns]	F [kHz]
A	1.5	6.8	167	75	10.33	0.88	1.23	1.38	9.8
B	2.5	15.2	177	92	8.0	0.89	1.22	1.45	9.8
C	3.2	20.7	179	92	6.25	0.89	1.20	1.35	9.8

TABLE IV

The optimal parameters of Nd:YAG/Cr:YAG microchip laser.

Data set	Optimization parameters			Laser radiation parameters			
	l_a [μm]	R_2	P_p [W]	P_{max} [kW]	E [μJ]	t_i [ns]	F [kHz]
A	140	0.97	2.5	1.6	0.86	0.54	9.6
B	140	0.97	2.5	1.4	0.84	0.60	9.8
C	140	0.97	2.5	1.3	0.75	0.58	9.9

4. Conclusions

The problem of the Q-switched microchip Nd^{3+}:YAG/Cr^{4+}:YAG laser optimization is considered. In accordance with requirements of rangefinder applications it consists in determination of such values of the absorber (Cr^{4+}:YAG) thickness l_a, the output laser mirror reflectivity R_2 and the pumping power P_p that ensure the generation of sufficiently short laser pulses ($t_i \approx 0.5$ ns) at the repetition rate F of about 10 kHz and peak power P_{max} of about 1 kW or higher. Firstly, based on the Xiao–Bass model of Q-switched microchip laser, we analyze the dependences of the laser radiation characteristics on the construction parameters. As it follows from our calculations, increase of the absorber thickness and/or the output mirror reflectivity leads to shortening of the laser pulse. On the other hand, increase of P_p leads to increase of the repetition rate without significant changes of other parameters of the pulse. In that way, the optimization consists in: (a) ensuring the value of t_i by variation of l_a and R_2, and (b) ensuring the value of F by variation of P_p. The values of the peak power P_{max} and the energy E remain in the allowable limits during the optimization and, accordingly, do not need any additional adjustment. Because of uncertainty of the absorption cross-sections of the active Cr^{4+} ions, the optimization was carried out for three data sets with different values of cross-sections of ground state and excited absorption state of phototropic Cr^{4+}(tetra) centers. As it is shown, the parameters of the laser radiation close to the predominating ones are achieved at the absorber thickness of 140 μm, the output mirror reflectivity of 0.97 and the pumping power of 2.5 W, for all considered data sets.

References

[1] G. Xiao, M. Bass, *IEEE J. Quantum Electronics* **33**, 2286 (1997).

[2] T. Dascalu, G. Philipps, H. Weber, *Opt. Laser Technol.* **29**, 145 (1997).

[3] Z. Mierczyk, *Non–linear absorbers*, Wojskowa Akademia Technichna, Warszawa 2000 (in Polish).

[4] O. Svelto, *Principles of Lasers*, New York-London 1998.

[5] G.M. Zverev, Ju.D. Goliajev, E.A. Shalaev, A.A. Shokin, *Lasers on the aluminium yttrium garnet with neodymium*, "Radio i svias", Moscow 1985 (in Russian).

[6] O.A. Buryy, S.B. Ubiszkii, S.S. Melnyk, A.O. Matkovskii, *Appl. Phys. B: Lasers and Optics* **78**, 291 (2004).

[7] R. Feldman, Y. Shimony, Z. Burshtein, *Opt. Mater.* **24**, 393 (2003).

[8] Y. Kalisky, A. Ben-Amar Baranga, Y. Shimony, M.R. Kokta, *Opt. Mater.* **8**, 129 (1997).

[9] A.G. Okhrimchuk, A.V. Shestakov, *Phys. Rev. B* **61**, 988 (2000).

[10] J.J. Zayhowski, A. Wilson, Jr., *IEEE J. Quantum Electronics* **39**, 1588 (2003).

[11] K. Kopczyński, Z. Mierczyk, M. Kwaśny, J. Mlyńczak, A. Gietka, J. Sarnecki, J. Skwarcz, in: *Int. Conf. Solid State Crystals — Materials Science and Applications, Book of Abstracts*, Zakopane, Poland 2002, p. 203.

[12] O.A. Buryy, S.B. Ubiszkii, S.S. Melnyk, A.O. Matkovskii, in: *Proc. Third Int. Workshop on Laser and Fiber-Optical Networks Modeling, Kharkiv, Ukraine*, 2001, p. 126.